Scanning Tunneling Microscopy and Spectroscopy Studies of Porphyrins at Solid–Liquid Interfaces

Bas Hulsken, Richard van Hameren, Pall Thordarson[1], Jan W. Gerritsen, Roeland J. M. Nolte, Alan E. Rowan, Maxwell J. Crossley[1], Johannes A. A. W. Elemans[*] and Sylvia Speller[†]

Institute for Molecules and Materials, Radboud University Nijmegen, Toernooiveld 1, 6525 ED Nijmegen, The Netherlands
[1]*School of Chemistry, The University of Sydney, NSW 2006, Australia*

Monolayers of two tetrakis(*meso*-undecyl)porphyrins adsorbed at the interface of a liquid and highly oriented pyrolytic graphite (HOPG) and Au(111) surfaces have been investigated with scanning tunneling microscopy (STM). Both molecules form stable monolayers on these surfaces, and topographic images have been obtained down to the submolecular level. For the first time, scanning tunneling spectroscopy (STS) has been used to reveal the electronic properties of this type of molecules at a solid–liquid interface. [DOI: 10.1143/JJAP.45.1953]

KEYWORDS: solid–liquid interfaces, scanning tunneling microscopy, scanning tunneling spectroscopy, surface electronic phenomena, interface states, gold, alkanes, porphyrins, chromophores

1. Introduction

The organization of functional molecules into highly organized arrays is an area of research with great potential application in material sciences.[1] Tunneling experiments through individual molecules in such arrays can give vital information about their electronic properties. (Metallo)porphyrins are particularly attractive molecules for the construction of such arrays, because they can be used as building blocks for (photo)catalytic, electronic and magnetic materials.[2,3] The construction of nanosized porphyrin assemblies by spontaneous self-assembly of the molecules is an attractive alternative for the construction of porphyrin arrays by multistep and time-consuming covalent synthesis. Several examples of porphyrin arrays self-assembled at a solid–liquid interface have been reported, and the assemblies have been characterized down to the (sub)molecular level with the help of scanning tunneling microscopy (STM).[4–6] Most STM studies on porphyrins have been carried out on tetrakis(*meso*-phenyl) derivatives. However, since in these molecules the *meso*-phenyl rings define an angle of about 60° with the central porphyrin plane, it can be expected that upon adsorption the center of the porphyrin, where the active metal-binding site is located, cannot have a strong interaction with the underlying surface. In terms of function of the molecules, a strong interaction with the surface might be desired since in such way the electronic properties of the active center can be studied and, ideally, controlled.

We have therefore prepared porphyrins **H₂1** and **Cu1**, which have four undecyl chains as *meso*-substituents (Fig. 1). Molecular modeling calculations reveal that these molecules can adopt a completely flat shape. We here present STM studies of monolayers of these molecules at solid–liquid interfaces, and for the first time scanning tunneling spectroscopy (STS) studies on this type of molecule at such an interface will be reported.

2. Experimental

The synthesis of **H₂1** and **Cu1** will be described elsewhere. STM measurements were carried out in the constant
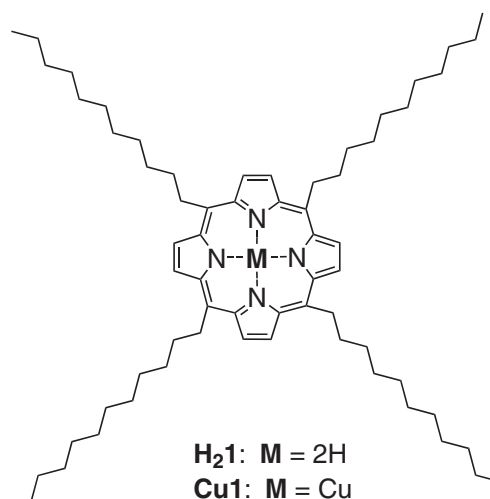

Fig. 1. Chemical structure of porphyrin molecules **H₂1** and **Cu1**.

current mode using a home-built low-current STM. STM tips were mechanically cut from a $Pt_{80}Ir_{20}$ wire. For the experiments on highly oriented pyrolytic graphite (HOPG), the surface was freshly cleaved before each measurement. A drop of a nearly saturated solution of the molecules in 1-phenyloctane was brought to the surface. Before and after the experiments the piezo was calibrated *in situ* by lowering the bias voltage to 100 mV and raising the tunnelling current to 50 pA, which allowed imaging of the HOPG surface underneath the molecules. Typically, an STM image (1024 lines 1024 points) was recorded over a period of 10 minutes. The STM raw data were processed only by the application of a background flattening. The STM and STS measurements on Au(111) were performed with the home built *Nijmegen Liquid-Cell STM* and an Omicron SCALA SPM controller. Measurements were done on fresh Au(111) films mounted in a liquid cell filled with argon bubbled tetradecane. The complete STM was enclosed in a bell-jar with an argon atmosphere. The Au(111) films were prepared in an evaporator using 99.99% gold and freshly cleaved mica. The gold was grown epitaxially on the heated mica (~300 °C), at a pressure of 10^{-7} mbar, and annealed for 2 h at 300 °C, 10^{-8} mbar. Immediately before mounting the

*E-mail address: J.Elemans@science.ru.nl
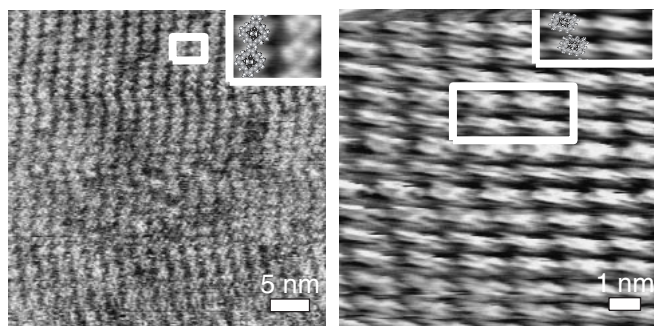†E-mail address: S.Speller@science.ru.nl

Fig. 2. (a) Constant current image ($I = 50$ pA, $V = -800$ mV) of a self-assembled monolayer of $H_2 1$ on HOPG. The inset shows a correlation averaged 3 times enlarged zoom-in, with the proposed molecular orientation drawn in. (b) Constant current image ($I = 28$ pA, $V = -223$ mV) of a self-assembled monolayer of **Cu1** on HOPG. The inset shows a correlation average, with the proposed molecular orientation drawn in. This image looks compressed in the vertical direction due to (thermal) drift during the measurement. In reality the molecules have a more square lattice as in the left (a). In both figures, the molecular models are drawn without alkyl-tails because their precise orientation can not be determined from the STM data.
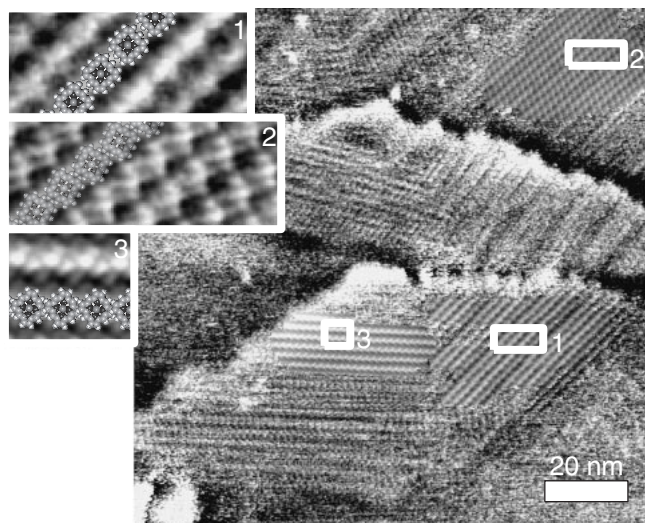

Fig. 3. Constant current image ($I = 15$ pA, $V = -200$ mV) of a self-assembled monolayer of **Cu1** on Au(111). The insets (1 to 3) show correlation averaged, and 5 times enlarged zoom-ins of the different structures of the **Cu1** porphyrin monolayer on the gold. The same correlation averaging is applied to the three different domains in the full image. In the insets, the proposed molecular ordering is drawn in. The molecular models are drawn without alkyl-tails because their precise orientation can not be determined from the STM data.

film in the liquid cell, the film was annealed in a hydrogen flame. The tetradecane (Aldrich, 99+%) was purified by distillation and degassed by bubbling with argon for several hours.

3. Results and Discussion

A drop of a nearly saturated solution of $H_2 1$ in 1-phenyloctane was brought onto the basal plane of freshly cleaved HOPG. Instantaneously, STM images showed the presence of extended arrays of the porphyrin at the solid–liquid interface [Fig. 2(a)]. The well-defined pattern of bright and dark areas, respectively, corresponds to the aromatic cores of the porphyrins and the aliphatic parts of the molecules of $H_2 1$.[7] The size of each of the bright areas (12×12 Å^2) is in good agreement with the dimensions of the aromatic plane of the porphyrin. These planes could be imaged with submolecular resolution, and appeared to consist of four bright spots surrounding a dark hole in the center. These spots might correspond to the four pyrrolic units of the porphyrin. STM images of **Cu1** at the interface of HOPG and 1-phenyloctane showed arrays of porphyrins similar to those observed for $H_2 1$ [Fig. 2(b)]. However, the resolution within the porphyrin planes of **Cu1** is less clear than that in $H_2 1$ and a dark spot in the center appears absent. This effect is attributed to the absence or presence of metal centers in the porphyrins, which is known to have a pronounced influence on the tunneling resistance.[8] Both porphyrins are arranged in a lamellar structure, where the alkyl chains are located on both sides of the arrays of closely packed aromatic planes. Cu(II) phthalocyanine derivatives on HOPG were found to arrange in a lamellar structure with a bright metal center,[9] similar to the structure observed here for **Cu1** in Fig. 2(b), whereas freebase tetrakis-*meso*-substituted porphyrins were found to arrange in lamellar structures with dark cores,[10] similar to what was observed here for $H_2 1$ in Fig. 2(a).

The organization of **Cu1** and $H_2 1$ was also investigated at another solid–liquid interface, *viz.* that of Au(111) and *n*-

tetradecane. It has previously been established that at this interface one can perform reliable scanning tunneling spectroscopy, and that the interface is free of contaminations such as oxygen and water.[11] As on HOPG, **Cu1** instantaneously assembles in extensive arrays at the solid–liquid interface, leading to nearly full surface coverage (Fig. 3). The domains of **Cu1** on Au(111) are smaller than on HOPG, and can have different orientation and structure (see insets in Fig. 3). The different orientations are due to the 6-fold symmetry of the Au(111) surface. The insets in Fig. 3 show the three apparently unique packing arrangements in the full image. The domain below region 3 is a rotational domain of region 1, the domain above region 3 is a rotational domain of region 2. The different structure can be tentatively explained by interference with the $23 \times \sqrt{3}$ reconstruction of the Au(111). This reconstruction is known to be present at this interface, and the STM topography shows some indications that it prevails, in spite of the adsorption of the porphyrins; most notably one can see some banding in the right side of the image, at and above the square marked 1. These bands are approximately 5 nm wide, which matches the unit cell of the $23 \times \sqrt{3}$ reconstruction. STM measurements during the formation of the **Cu1** monolayer, which will be described elsewhere, also indicate the preservation of the reconstruction under the monolayer. Similar to **Cu1** on HOPG, the porphyrins have a bright core, which corresponds to the aromatic plane of the molecule, the alkyl tails are in the dark areas surrounding the bright core. Attempts to image the $H_2 1$ adsorbed at the Au(111)/tetradecane interface failed, in spite of numerous attempts. It is proposed that the metal center plays a role in the binding of the molecule to the gold. This is supported by the observation that besides **Cu1**, porphyrins with a different metal center (Pt, Ni) bind to Au(111). The nature of the influence of the metal center
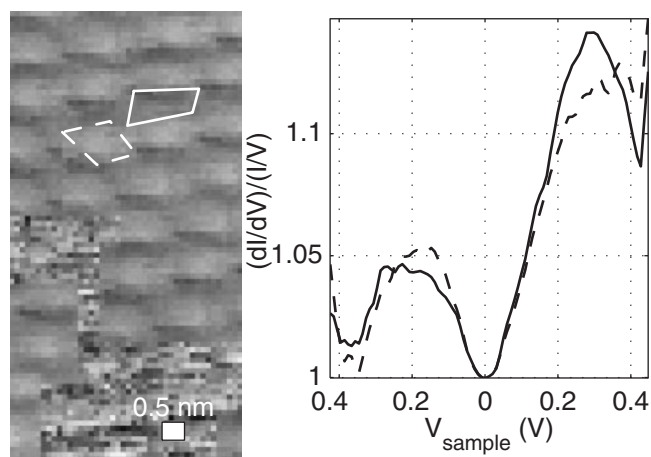
Fig. 4. Constant current image with simultaneous STS ($I = 200$ pA, $V = 500$ mV, voltage sweep $V = 500 \rightarrow -500$ mV) of **Cu1** on Au(111). Correlation averaging is applied to both the topography and spectroscopy data. The right hand side shows two spectroscopy curves, one on top of the porphyrin center (dashed) and one in between the porphyrin centers (solid). Two interface states are present in this energy range, one at -175 meV, and one at 300 meV.

4. Conclusions

We have found that **H₂1** and **Cu1**, which have four undecyl chains as *meso*-substituents, spontaneously self assemble into extended arrays on an HOPG surface in a droplet of 1-phenyloctane. The presence of a metal in the center of the porphyrin was found to have a large effect on the apparent topography: the "empty" **H₂1** has a dark core, while the 'metal filled' **Cu1** has a bright core.

In contrast with the HOPG/1-phenyloctane interface, at the Au(111)/*n*-tetradecane interface, the empty **H₂1** porphyrin does not form arrays at the interface, while the filled **Cu1** porphyrin does. It was found that also porphyrins with different metal centers (Pt, Ni) form arrays. This could indicate that the metal center is involved in the adsorption of these flat porphyrins to Au(111). Further investigation of the **Cu1** self-assembled monolayer on Au(111) with scanning tunneling spectrocopy indicates the presence of two interface states near the Fermi energy. Given the large HOMO–LUMO gap of the **Cu1**, one or both of these could tentatively be designated as binding states of the porphyrin to the Au(111).

Our ability to perform STM/STS, both with molecular resolution, on these self-assembled monolayers of porphyrins provides a wealth of information regarding structure and electronic properties. This might in the future lead to a detailed understanding of the binding mechanisms of porphyrins to metals, which can lead to better control of the active metal center of the porphyrins.

might be a redox reaction, as has been observed for Zn(II) porphyrins and Zn(II) phthalocyanines.[12] That the **H₂1** porphyrin binds to HOPG and not to Au(111) can be explained by the stronger binding of the alkyl-tails to HOPG.

The monolayer of **Cu1** porphyrins was stable enough to perform scanning tunneling spectroscopy. Normalized differential conductivity curves, i.e., $(dI/dV)/(I/V)$ curves, are shown in the right part of Fig. 4. The spectroscopy curves were taken with the feedback off, and simultaneously with a STM constant current topography measurement. The experimental data so obtained consist of a topography image, with for each point of the topography a current-voltage, $I(V)$, curve. The STM topography has molecular resolution (lefthand side of Fig. 4) and the unit cell found from the topography image was used to filter the spectroscopy data. This filter method uses correlation to find the unit-cell in the topography image, and averages the spectroscopy curves over this unit cell.[13] In this manner, the noise in the spectroscopy data is significantly reduced, resulting in spectroscopy data with molecular resolution. From the spectroscopy data one can see that two states are present around the Fermi energy. The state at ~ -175 meV is more pronounced on the center of the porphyrin, while the state at ~ 300 meV is more pronounced in between the aromatic centers. The origin of these states remains yet to be explained. The Au(111) has a surface state at ~ -500 meV, which doesn't shift significantly at the Au(111)/*n*-tetradecane interface.[11] The homo-lumo gap of the **Cu1** porphyrin is rather large (HOMO at -2.06 eV, LUMO at -4.86 eV); which makes it unlikely, although not impossible, to find two molecular orbitals this close to the Fermi energy. In the light of this, it seems reasonable to designate one or both of these states as (anti-) binding states between the Au(111) and the metal center of the porphyrin.

1) J.-M. Lehn: Science **295** (2002) 2400.
2) C.-Y. Liu, H.-I. Pan, M. A. Fox and A. H. Bard: Science **261** (1993) 897.
3) K. S. Suslick, N. A. Rakow, M. E. Kosal and J.-H. Chou: J. Porphyrins Phthalocyanines **4** (2000) 407.
4) T. A. Jung, R. R. Schlittler, J. K. Gimzewski, H. Tang and C. Joachim: Science **271** (1996) 181.
5) L. Scudiero, D. E. Barlow and K. W. Hipps: J. Phys. Chem. B **106** (2002) 996.
6) X. Qiu, C. Wang, Q. Zeng, B. Xu, S. Yin, H. Wang, S. Xu and C. Bai: J. Am. Chem. Soc. **122** (2000) 5550.
7) R. Lazzaroni, A. Calderone, J. L. Bredás and J. P. Rabe: J. Chem. Phys. **107** (1997) 99.
8) L. Scudiero, D. E. Barlow and K. W. Hipps: J. Phys. Chem. B **104** (2000) 11899.
9) S. B. Lei, S. X. Yin, C. Wang, L. J. Wan and C. L. Bai: Chem. Mater. **14** (2002) 2837.
10) J. Otsuki, E. Nagamine, T. Kondo, K. Iwasaki, M. Asakawa and K. Miyake: J. Am. Chem. Soc. **127** (2005) 10400.
11) B. Hulsken, J. W. Gerritsen and S. Speller: Surf. Sci. **580** (2005) 95.
12) S. Yoshimoto, E. Tsutsumi, K. Suto, Y. Honda and K. Itaya: to be published in Chem. Phys.
13) B. Hulsken, J. W. Gerritsen and S. Speller: unpublished.